Front. Med. 2019, 13(2): 267–276
https://doi.org/10.1007/s11684-017-0586-8

RESEARCH ARTICLE

Preventive effect of Shenkang injection against high glucose-induced senescence of renal tubular cells

Biqiong Fu*, Jie Yang*, Jia Chen, Lirong Lin, Kehong Chen, Weiwei Zhang, Jianguo Zhang, Yani He (✉)

Department of Nephrology, Daping Hospital, Army Medical University, Chongqing 400042, China

Abstract **Shenkang injection (SKI) is a classic prescription composed of *Radix Astragali*, rhubarb, *Astragalus, Safflower*, and *Salvia*. This treatment was approved by the State Food and Drug Administration of China in 1999 for treatment of chronic kidney diseases based on good efficacy and safety. This study aimed to investigate the protective effect of SKI against high glucose (HG)-induced renal tubular cell senescence and its underlying mechanism. Primary renal proximal tubule epithelial cells were cultured in (1) control medium (control group), medium containing 5 mmol/L glucose; (2) mannitol medium (mannitol group), medium containing 5 mmol/L glucose, and 25 mmol/L mannitol; (3) HG medium (HG group) containing 30 mmol/L glucose; (4) SKI treatment at high (200 mg/L), medium (100 mg/L), or low (50 mg/L) concentration in HG medium (HG + SKI group); or (5) 200 mg/L SKI treatment in control medium (control + SKI group) for 72 h. HG-induced senescent cells showed the emergence of senescence associated heterochromatin foci, up-regulation of $P16^{INK4}$ and cyclin D1, increased senescence-associated β-galactosidase activity, and elevated expression of membrane decoy receptor 2. SKI treatment potently prevented these changes in a dose-independent manner. SKI treatment prevented HG-induced up-regulation of pro-senescence molecule mammalian target of rapamycin and p66Shc and down-regulation of anti-senescence molecules klotho, sirt1, and peroxisome proliferator-activated receptor-γ in renal tubular epithelial cells. SKI may be a novel strategy for protecting against HG-induced renal tubular cell senescence in treatment of diabetic nephropathy.**

Keywords Shenkang injection; senescence; renal tubular epithelial cells; diabetic nephropathy

Introduction

Diabetic nephropathy (DN) is one of the most common complications of diabetes and is also the most frequent cause of end-stage renal disease. Renal proximal epithelial tubular cells are fragile parenchyma cells that are susceptible to hypoxia- and oxidative stress-induced injury in a high-glucose (HG) metabolic environment. Injured epithelial tubular cells initially exhibit hyperplasia and hypertrophy and finally experience stress-induced premature senescence [1]. Recent studies have shown that renal tubular epithelial cell senescence occurs in renal tissues of both DN patients and a diabetic rat model even at an early stage [2–4]. *In vitro* experiments also confirmed that HG accelerates stress-induced premature senescence of renal tubular epithelial cells, indicating renal tubular cell senescence as an important biological event in tubulointerstitial injury during DN progression [5]. Renal tubular cell senescence has also been found to be closely associated with tubular atrophy, interstitial inflammation, interstitial fibrosis, and renal function failure. Accelerated senescence of renal tubular epithelial cells confers high susceptibility to renal injury and impedes renal repair through inhibition of tubular cell proliferation [6,7]. As stress-induced premature senescence in renal tubular cells plays an important role in DN progression, prevention and treatment of renal tubular cell senescence may offer a novel therapeutic approach to prevention and retardation of DN.

Shenkang injection (SKI) with certification No. Z20040110 was approved by the State Food and Drug Administration of China in 1999 for treatment of chronic kidney diseases (CKD) (Permission No. YBZ08522004). This treatment is a classic prescription comprising four medicinal crude drugs, including Radix et Rhizoma Rhei (Dahuang in Chinese, RRR, *Rheum palmatum* L.), Radix

Received December 22, 2016; accepted August 15, 2017
Correspondence: Yani He, heynmail@163.com

*These authors have contributed equally to this work.

et Rhizoma Salviae Miltiorrhizae (Danshen in Chinese, SMRR, *Salvia miltiorrhiza* Bge.), Radix Astragali (Huangqi in Chinese, AR, *Astragalus membranaceus* (Fisch.) Bunge), and Flos Carthami (Honghua in Chinese, CF, *Carthamus tinctorius* L.). SKI is manufactured by Xi'an Shiji Shengkang Pharmaceutical Industry Co., Ltd. The injection includes a yellow-brown, clear liquid, 20 ml × 5-piece set, and each contains 6 g crude drug extracts. A prospective, phase IV multi-center clinical study of 2200 patients with CKD at stages 3–4 demonstrated significant improvements in decreasing serum creatinine and creatinine clearance 1–3 months after treatment with SKI. A total of 73.05% of patients exhibited improved renal function, and 98.00% presented alleviated clinical symptoms, suggesting good efficacy and safety of SKI in treatment of CKD [8–10]. Both *in vitro* and *in vivo* studies have shown that SKI significantly inhibits oxidative stress-induced renal injury and prevents interstitial fibrosis [11]. SKI also effectively attenuates HG-induced mesangial cell hypertrophy through inhibition of P21 overexpression, thus preventing HG-induced senescence in mesangial cells [12]. Although SKI has been reported to play a beneficial role in minimizing renal injury and expediting tissue repair, little is known about its effects on renal proximal epithelial tubular cells. In this study, we investigated potential protective effects of SKI against HG-induced renal tubular cell senescence and its underlying mechanism.

Materials and methods

Reagents and antibodies

SKI was purchased from Xi'an Shiji Shengkang Pharmaceutical Industry Co., Ltd. (Xi'an, China). Production process of SKI was subjected to strict quality control, and the main components were standardized [13]. Fig. 1 shows high-performance liquid chromatography (HPLC) of SKI used in the study. SKI is not only manufactured as injection after dynamic cycle extraction and concentration but also monitored for the absence of contaminants (heavy metals, pesticides, hormones, and mycotoxins) prior to formulation. Table 1 summarizes the batch number and quality control data of SKI. Anthraquinone content of Radix et Rhizoma Rhei reached 2.5%, whereas that of astragaloside IV in Radix Astragali totaled 0.119%. Glucosinolate content of isoflavones was 0.111%, tanshinone content of Radix et Rhizoma Salviae Miltiorrhizae was maintained at 0.45%, whereas salvianolic acid B content accounted for 7.5% of total compounds. Kaempferol content reached 0.116%, and content of hydroxysafflor yellow A remained at 2.4%.

A total of 20% mannitol, 50% glucose, Dulbecco's modified Eagle's medium, F12 medium, and fetal bovine serum were purchased from Gibco (Grand Island, NY, USA). Epidermal growth factor, insulin transferrin selenium sodium pyruvate, and Trizol were obtained from Invitrogen (Carlsbad, CA, USA). Bovine serum albumin and essential amino acids were purchased from Sigma-Aldrich (St. Louis, MO, USA). Type II collagen enzyme was purchased from Worthington (Lakewood, NJ, USA). Reverse transcription polymerase chain reaction (RT-PCR) kit and SYBR Green® were purchased form Takara (Shiga, Japan). Senescence-associated β-galactosidase (SA-β-Gal) staining kit came from Beyotime Biotechnology (Jiangsu, China). Antibodies against $P16^{INK4}$, klotho, sirt1, peroxisome proliferator-activated receptor (PPAR-γ), cytokeratin 18 (CK18), β-actin, and mammalian target of rapamycin (mTOR) were purchased from Santa Cruz Biotechnology (Santa Cruz, CA, USA). An antibody against P66shc and polyvinylidene difluoride (PVDF) membrane were obtained from Millipore (Bedford, MA, USA). An antibody against villin was obtained from Abcam (Cambridge, MA, USA). A reactive oxygen species (superoxide dismutase, SOD) detection assay kit

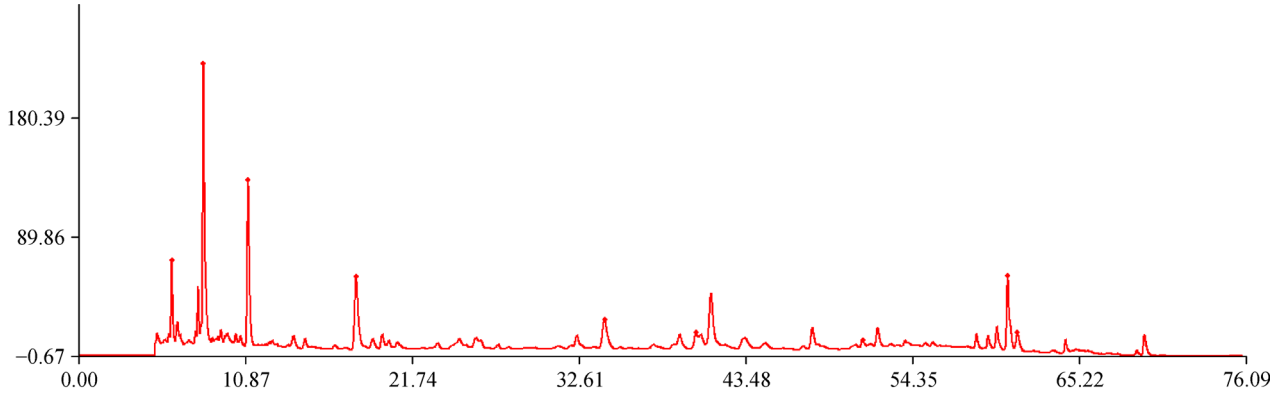

Fig. 1 HPLC of SKI used in the study. The main compounds of SKI include gallic acid, salvianic acid, protocatechualdehyde, propanoid acid, hydroxysafflor yellow A, emodin-O-glucoside, and salvianolic acid.

and a lipid peroxidation (malondialdehyde, MDA) assay kit were purchased from Nanjing Jiancheng Bioengineering Institute (Nanjing, China).

Cell culture

Renal cortex tissues were obtained form 3-week-old male C57/BL6 mice under sterile conditions. All experiments were approved by the Army Medical University experiment animal administrative committee. All efforts were exerted to minimize suffering and reduce the number of animals used. Tissues were digested with type II collagenase and passed through a screen filter to isolate primary renal proximal tubule epithelial cells [14–16]. Expressions of specific renal tubular epithelial cell markers CK18 and villin were examined by immunofluorescence analysis. Cells from the second passage were cultured in serum-free medium for 24 h and then subjected to (1) control medium (control group), medium containing 5 mmol/L glucose; (2) mannitol medium (mannitol group), medium containing 5 mmol/L glucose, and 25 mmol/L mannitol; (3) HG medium (HG group) containing 30 mmol/L glucose; (4) SKI treatment at high (200 mg/L), medium (100 mg/L), or low (50 mg/L) concentrations of HG medium (HG + SKI group); or (5) 200 mg/L SKI treatment in control medium (control + SKI group). Cells were cultured for 72 h, and morphology was examined under an inverted microscope.

Immunofluorescence assay

Cells were collected and fixed on glass slides. After blocking with goat serum, the slides were incubated with primary antibodies against CK18 (1:200), villin (1:100), $P16^{INK4}$ (1:100), cyclin D1 (1:100), and decoy receptor 2 (DcR2) (1:100) at 4 °C overnight. After rinsing with phosphate-buffered saline, the slides were incubated with secondary antibodies at room temperature for 1 h. Cells were counterstained with Hoechst to visualize nuclei. Images were captured by a laser confocal microscope (Leica, Wetzlar, Germany).

SA-β-Gal staining and measurement of reactive oxygen species

Cells were collected and fixed in a six-well plate. Then, cells were stained using a SA-β-Gal staining kit according to manufacturer's instructions and were observed under an optical microscope. MDA content and SOD activity were determined according to manufacturer's instructions.

Western blot analysis

Cells were collected and lysed on ice. The supernatant was collected, and total proteins were quantified by bicinchonic acid method. Protein samples were loaded onto polyacrylamide gels and subjected to sodium dodecyl sulfate polyacrylamide gel electrophoresis. Proteins were then electroblotted onto a PVDF membrane. The membrane was blocked with 5% fat-free milk at room temperature for 2 h, followed by incubation with primary antibody (mTOR, P66shc, klotho, sirt1, or PPAR-γ (diluted at 1:1000; β-actin as control, diluted at 1:1000)) at 4 °C overnight. After washing, membranes were incubated at room temperature for 1 h with secondary antibodies. The membranes were washed with Tris-buffered saline-Tween 20. Then, density of corresponding bands was measured quantitatively using image analysis software (Quantity One, Bio-Rad Laboratories, Hercules, CA, USA) and corrected by reference to the value for β-actin.

Table 1 Batch number and quality control data of SKI

Name	Batch number	Dose	pH value	Residue on ignition (%)	Total solids (mg/mL)	Total anthraquinone (μg/mL)	Total sugar (mg/mL)	Polysaccharide (mg/mL)	Emodin chrysophanol (μg/mL)
Shenkang injection	201405041	20 mL	6.7	0.1	18.9	60	11.3	7.2	21
Shenkang injection	201405042	20 mL	6.7	0.2	17.8	60	10.9	6.7	21
Standard regulation			5.0–7.0	<0.5%	>14.0 mg	>50 μg	>8.0 mg	>4.0 mg	>8 μg

Name	Batch number	Pyrogenic	Sterile	Heavy metals and toxic elements residue (μg)				
				Lead	Cadmium	Arsenic	Mercury	Copper
Shenkang injection	201405041	Compliance	Compliance	Not detected	0.22	1.83	Not detected	Not detected
Shenkang injection	201405042	Compliance	Compliance	Not detected	0.14	0.11	Not detected	Not detected
Standard regulation				<12 μg	<3 μg	<6 μg	<2 μg	<150 μg

Real-time PCR

Total RNA was extracted using Trizol reagent, and samples were reverse-transcribed into cDNA using a RT-PCR kit. Table 2 summarizes the primer sequences used for PCR analyses. Real-time PCR was performed with a Biorad CFX96 real-time PCR system (Applied Biosystems, Foster City, CA, USA). Thermal cycling conditions were as follows: 40 cycles of 95 °C for 30 s, 95 °C for 5 s, and 56 °C–63 °C for 40 s. A standard curve was constructed by using serial dilutions of a known template. Relative amount of mRNA of each sample was calculated using the $2^{-\Delta\Delta Ct}$ method.

Statistical analysis

Statistical analysis was performed using the SPSS software package (version 18.0; SPSS Inc, Chicago, IL, USA). Quantitative data are presented as mean ± standard deviation (SD). Data were analyzed using one-way analysis of variance to evaluate inter-group differences. $P < 0.05$ was considered statistically significant.

Results

SKI inhibits HG-induced senescence among renal tubular epithelial cells

Exposure to HG for 72 h but not to mannitol resulted in a flatter and larger cell morphology compared with control culture conditions. Interestingly, SKI treatment restored cells to nearly a normal shape, especially at a high concentration of 200 mg/L, suggesting that SKI improved HG-induced hypertrophy of renal tubular epithelial cells in a dose-dependent manner (Fig. 2A).

We determined the effect of SKI on expressions of senescence markers, including senescence-associated heterochromatin foci (SAHF), SA-β-Gal, $P16^{INK4}$, cyclin D1, and DcR2 in renal tubular epithelial cells. Compared with control cells, emergence of SAHF was observed in the HG group after culture for 72 h but not in the mannitol group. SKI effectively inhibited SAHF formation in a dose-dependent manner (Fig. 2B).

Upon SA-β-Gal staining, a significantly higher percentage of SA-β-Gal-positive cells was observed among HG-induced renal tubular epithelial cells, with an almost 4.6-fold increase compared with control cells ($P < 0.05$). However, SKI treatment resulted in a remarkably lower percentage of SA-β-Gal-positive cells in comparison with the HG group, especially in the 200 mg/L SKI group in which percentage of SA-β-Gal-positive cells was 86% less than that in the HG group ($P < 0.05$) (Fig. 2C and 2D).

Culture with HG resulted in an approximate 2.1-fold increase in percentage of $P16^{INK4}$-positive cells and 1.9-fold increase in the percentage of cyclin D1-positive cells compared with those in the control group ($P < 0.05$). SKI treatment significantly reduced the percentage of $P16^{INK4}$-positive cells and cyclin D1-positive cells, especially in the 200 mg/L SKI group in which the percentage of $P16^{INK4}$-positive cells was 58% lower than that in the HG group; cyclin D1-positive cells was 63% lower than that of the HG group ($P < 0.05$). By contrast, mannitol exerted no effect on the expression of $P16^{INK4}$ (Fig. 2E and 2F). Similarly, SKI can reverse HG-induced upregulation of cyclin D1 and DcR2 in a dose-dependent manner ($P < 0.05$ vs. HG group) (Fig. 2G, 2H, and 2I).

Anti-oxidative stress effect of SKI during HG-induced senescence

After exposure to HG for 72 h, renal tubular epithelial cells exhibited increased MDA content and decreased SOD activity compared with control cells ($P < 0.05$). SKI

Table 2 Primer sequences used for RT-PCR analysis

Genes	Primer sequences	Annealing temperature (°C)
Actin	5′ CATGGATGACGATATCGCTGC 3′	60
	5′ GTACGACCAGAGGCATACAGG 3′	
Sirt1	5′ GCTGACGACTTCGACGACG 3′	63
	5′ TCGGTCAACAGGAGGTTGTCT3′	
Klotho	5′ CAAAGTCTTCGGCCTTGTTC 3′	56
	5′ CTCCCCAAGCAAAGTCACA 3′	
PPAR-γ	5′ TGTCGGTTTCAGAAGTGCCTTG 3′	60
	5′ TTCAGCTGGTCGATATCACTGGAG 3′	
mTOR	5′ GCCACCTGGTATGAGAAGC 3′	63
	5′ CCAACACTGCCCTGTAAAA 3′	
P66shc	5′ CCGACTACCTGTGTTCCTTCTT 3′	60
	5′ CCCATCTTCAGCAGCCTTTCC 3′	

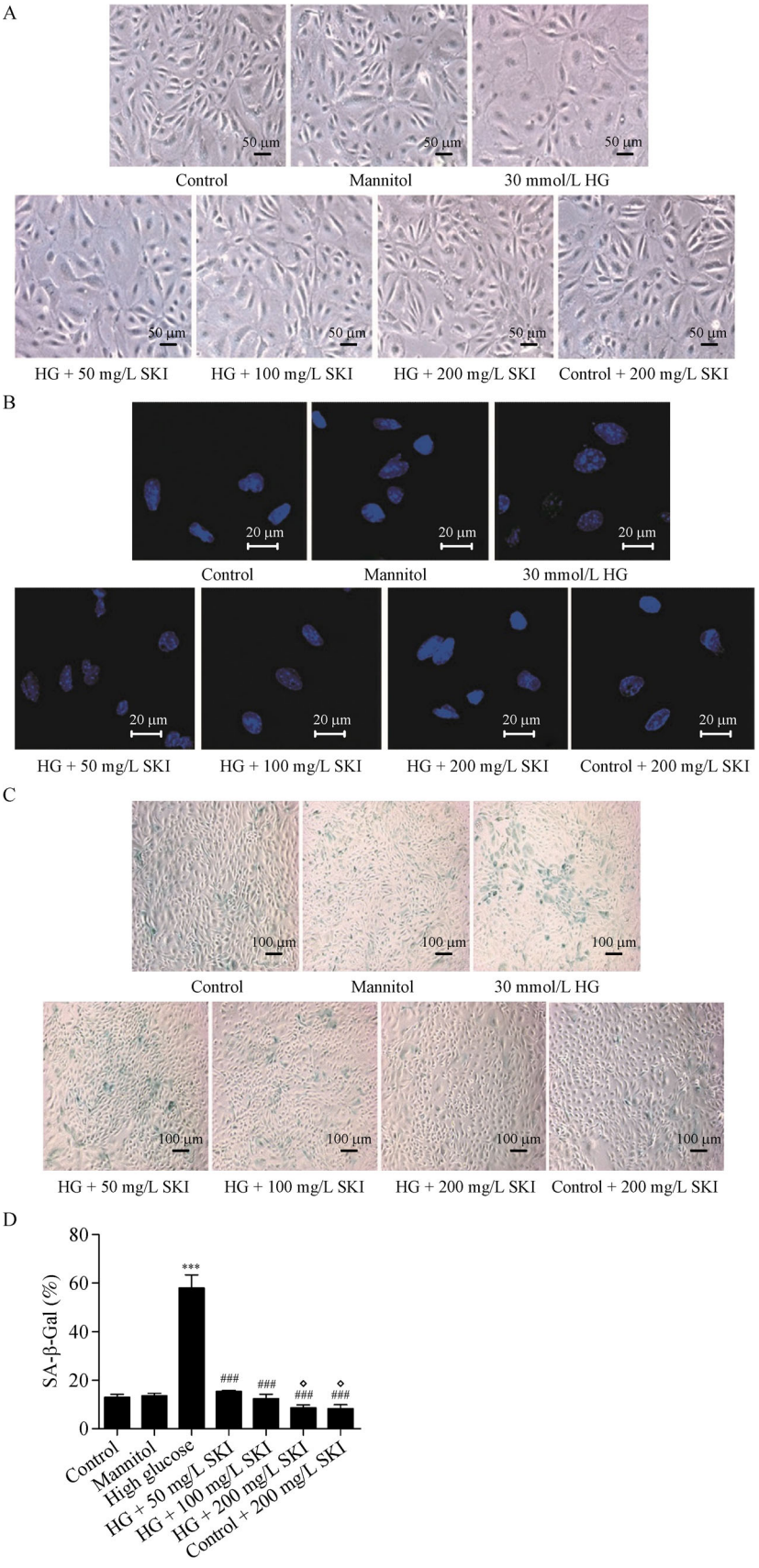
A
50 μm
Control
Mannitol
30 mmol/L HG
HG + 50 mg/L SKI
HG + 100 mg/L SKI
HG + 200 mg/L SKI
Control + 200 mg/L SKI
B
20 μm
Control
Mannitol
30 mmol/L HG
HG + 50 mg/L SKI
HG + 100 mg/L SKI
HG + 200 mg/L SKI
Control + 200 mg/L SKI
C
100 μm
Control
Mannitol
30 mmol/L HG
HG + 50 mg/L SKI
HG + 100 mg/L SKI
HG + 200 mg/L SKI
Control + 200 mg/L SKI
D
SA-β-Gal (%)
80
60
40
20
0
***
###
◇
Control
Mannitol
High glucose
HG + 50 mg/L SKI
HG + 100 mg/L SKI
HG + 200 mg/L SKI
Control + 200 mg/L SKI

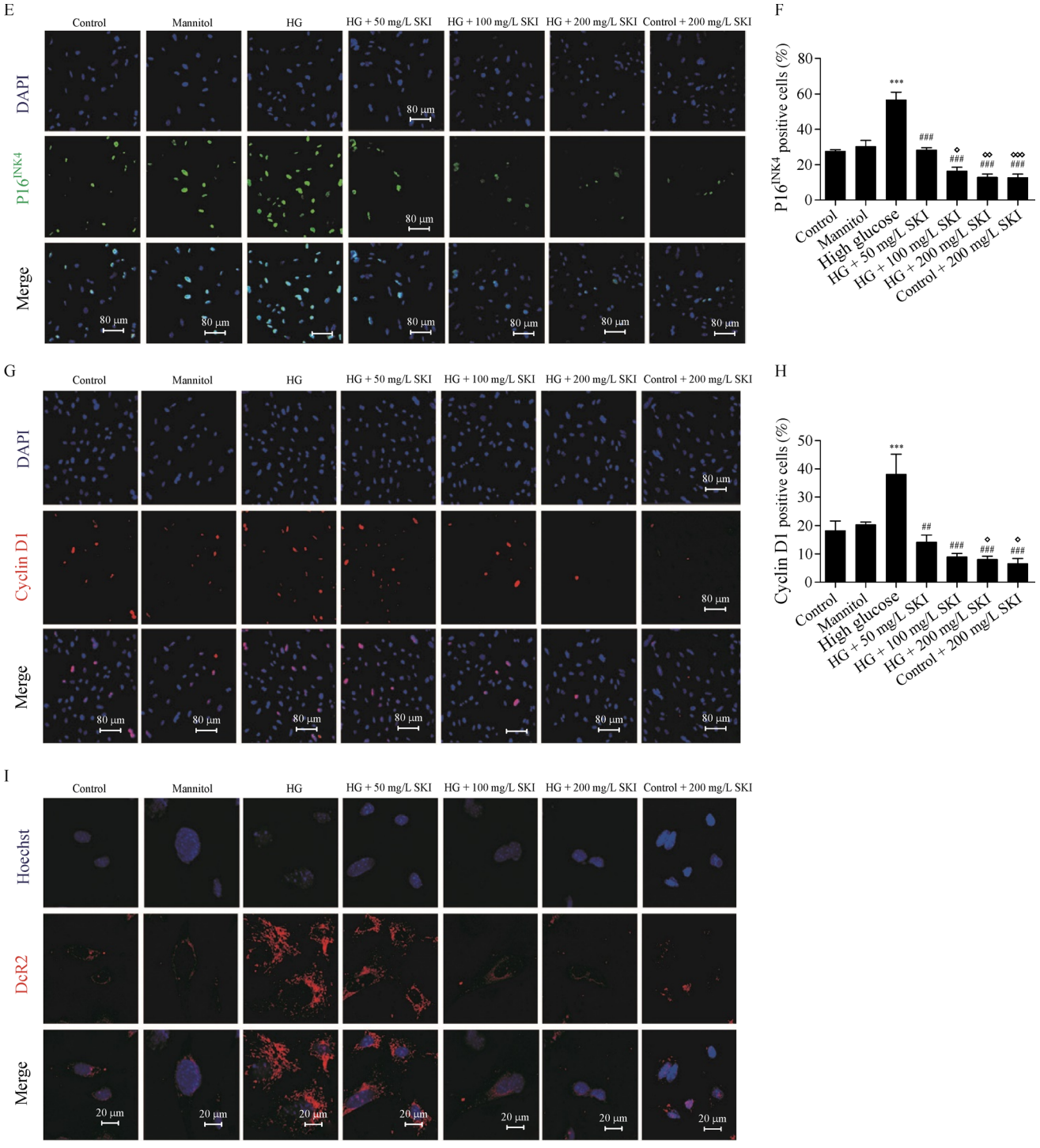

Fig. 2 Dose-dependent effect of SKI on expression of senescence markers in primary proximal tubular cells cultured under different conditions. (A) Cell morphology was examined under inverted microscopy after culturing for 72 h (magnification, 200×); (B) emergence of SAHF (magnification, 1200×); (C, D) SA-β-Gal staining and percentage of SA-β-Gal-positive cells (magnification, 100×); (E, F) expression of $P16^{INK4}$ in cell nuclei and quantitative analysis of $P16^{INK4}$-positive cells (magnification, 400×); (G, H) expression of cyclin D1 in cell nuclei and quantitative analysis of cyclin D1-positive cells (magnification, 400×); and (I) emergence of DcR2 in cytoplasm (magnification, 1200×). Values are mean ± SD of independent experiments with triplicate dishes. $^{*}P < 0.05$ vs. control; $^{**}P < 0.01$ vs. control; $^{***}P < 0.001$ vs. control; $^{\#}P < 0.05$ vs. HG group; $^{\#\#}P < 0.01$ vs. HG group; $^{\#\#\#}P < 0.001$ vs. HG group; $^{\diamond}P < 0.05$ vs. HG + SKI (50 mg/L); $^{\diamond\diamond}P < 0.01$ vs. HG + SKI (50 mg/L).

treatment effectively reduced HG-induced MDA production and increased SOD activity at all three concentrations tested in a dose-dependent manner (all $P < 0.05$ vs. HG group), suggesting that SKI plays a role in reducing oxidative stress in HG-exposed renal tubular epithelial cells (Fig. 3).

SKI inhibits expression of mTOR and P66shc

To investigate potential targets through which SKI inhibits HG-induced senescence, we detected expression of mTOR and P66shc at mRNA and protein levels. Results showed that mRNA levels of mTOR and P66shc in the HG group were elevated by 2.7- and 3.8-fold, respectively, compared with those in the control group (both $P < 0.05$). Also, protein levels of mTOR and P66shc were 2.2- and 2.9-fold higher in the HG group, respectively, than those in the control group (both $P < 0.05$). SKI treatment significantly reduced expressions of mTOR and P66shc at both mRNA and protein levels (all $P < 0.05$). These data revealed that SKI possibly inhibited HG-induced senescence by inhibiting mTOR and P66shc expressions (Fig. 4).

SKI promotes expressions of klotho, sirt1, and PPAR-γ

We also detected expressions of klotho, sirt1, and PPAR-γ at mRNA and protein levels in renal tubular epithelial cells. mRNA levels of klotho, sirt1, and PPAR-γ in the HG group accounted for 37%, 18.97%, and 50.6% of those in the control group, respectively (all $P < 0.05$). Similarly, protein levels of klotho, sirt1, and PPAR-γ in the HG group were reduced to 28%, 36%, and 45% of the levels observed in the control group, respectively (all $P < 0.05$). Interestingly, SKI treatment remarkably upregulated klotho, sirt1 and PPAR-γ expression at both the mRNA and protein levels (all $P < 0.05$), with mRNA expression reaching 1.78-, 9.17-, and 1.24-fold higher than corresponding levels in the control group, respectively. Protein expressions were 1.78-, 3.44-, and 1.53-fold higher than the levels in the control group, respectively (all $P < 0.05$).

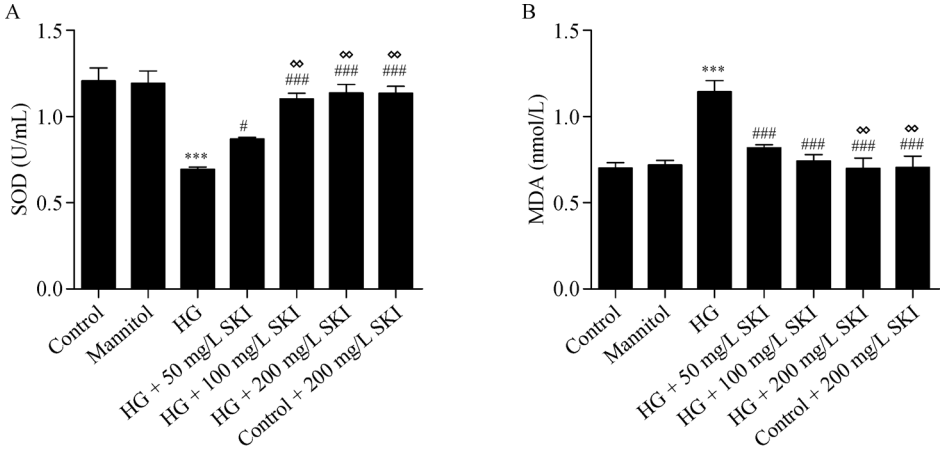

Fig. 3 Dose-dependent effect of SKI on SOD and MDA in renal tubular epithelial cells.

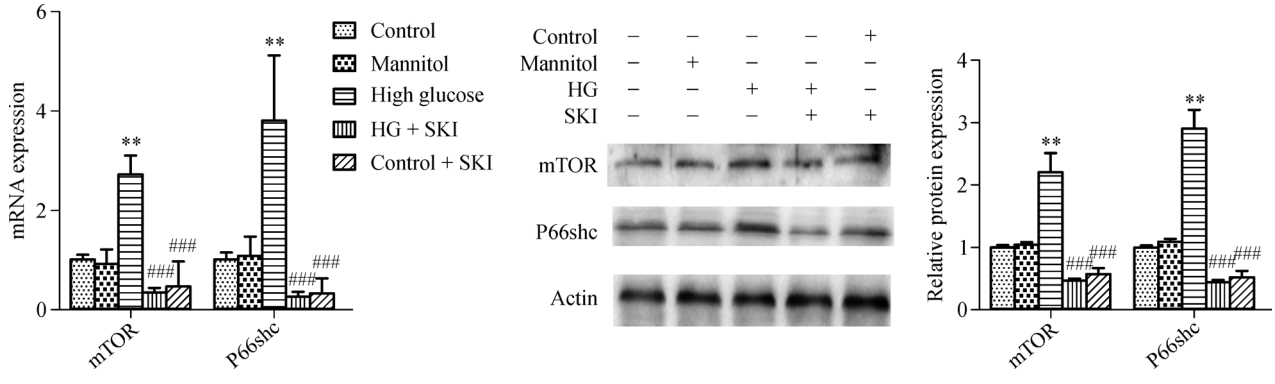

Fig. 4 Expression of mTOR and P66shc in renal tubular epithelial cells cultured under different conditions.

Thus, SKI inhibited HG-induced senescence possibly by upregulating klotho, sirt1, and PPAR-γ (Fig. 5).

Discussion

In diabetic state, renal tubular cells are directly exposed to a pathological microenvironment complicated by glucose and lipid metabolism disorders, persistent oxygen stress, and chronic inflammation at the very early stage, accelerating the occurrence of stress-induced senescence [17–21]. Morphologically, senescent cells appear flat and hypertrophic, with abnormal deposition of lipofuscin in the cytoplasm and heterochromatin aggregation in the nucleus, indicating formation of SAHF. Senescent cells show permanent stagnation of the cell cycle, upregulation of $P16^{INK4}$ and cyclin D1, increased SA-β-Gal activity, and elevated expression of membrane DcR2 [22]. Studies reported that DN is associated with acceleration of senescence among tubule cells in renal biopsy, and a similar senescent pattern was also observed for proximal tubule cells incubated in HG media *in vitro* [2]. Our study demonstrated that HG caused a flatter and larger cell morphology and emergence of SAHF. Also, senescence markers of SA-β-Gal activity, $P16^{INK4}$, cyclin D1, and DcR2 were upregulated in HG-exposed renal tubular epithelial cells. Interestingly, SKI significantly improved HG-induced renal tubular cell hypertrophy and reduced expression of $P16^{INK4}$, cyclin D1, and DcR2 and SA-β-Gal activity in a dose-dependent manner. Notably, SKI did not cause any abnormality in control cells, suggesting that SKI is non-toxic to normal cells.

In HG environment, mitochondrial energy metabolism disorder produces high amounts of reactive oxygen species, which in turn damage DNA and mitochondria, causing stress-induced senescence independent of age. *In vivo* studies have shown that SKI can significantly reduce the level of oxidative stress in kidneys and inhibit renal fibrosis [11,23]. HPLC analysis (HPLC fingerprints) has confirmed that SKI contains high amounts of potential antioxidant compounds [13]. *Astragalus membranaceus*, a main component of SKI, features an anti-senescence effect probably due to its properties as an antioxidant and regulator of telomerase activity [24]. Another important component of SKI is Radix et Rhizoma Rhei, which presents a potent antioxidant effect and can prolong survival of mice by reducing severity of renal lesions [25]. Notably, dosage of SKI used in clinical settings for treatment of chronic renal diseases reaches 6 g/L, whereas SKI concentration used in the present study was significantly lower than that in the plasma of patients. SKI inhibited HG-induced oxidative stress in renal tubular cells in a dose-dependent manner, and coincidentally, SKI was found to exert similar effects on HG-induced senescence. Thus, the effect of SKI on HG-induced tubular cell senescence can be attributed to its antioxidant capacity, indicating the mechanism of protective effects of SKI in early DN.

Renal cell senescence in DN is closely associated with activation of pro-senescence molecules, such as mTOR and P66Shc, and downregulation of anti-senescence molecules, including klotho, sirt1, and PPAR-γ [26–39]. Consistent with these findings, HG triggered upregulation of mTOR and P66Shc and downregulation of klotho, sirt1, and PPAR-γ in renal tubular epithelial cells. However, SKI potently reversed these changes by preserving balanced expression of pro-senescence and anti-senescence molecules, revealing synergistic effects of individual components of SKI for treatment of DN.

In conclusion, SKI may protect against HG-induced senescence among renal tubular epithelial cells by increasing expressions of anti-senescence molecules klotho, sirt1, and PPAR-γ and inhibiting levels of pro-senescence molecules mTOR and p66Shc. This study provides *in vitro* experimental evidence that SKI, as a classical traditional Chinese medicine prescription, may be a novel strategy for protecting against HG-induced renal tubular cell senescence in treatment of DN. However, the

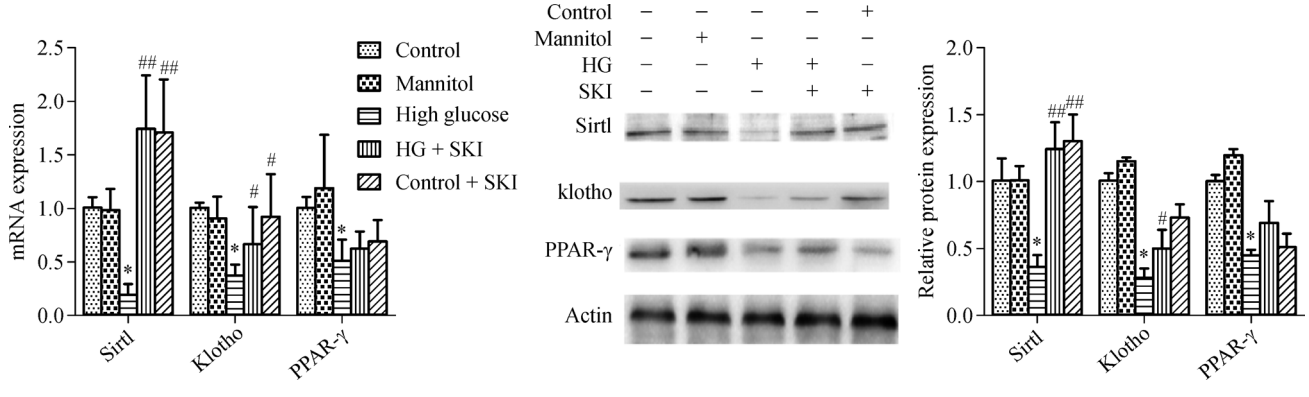

Fig. 5 Expression of klotho, sirt1, and PPAR-γ in renal tubular epithelial cells cultured under different conditions.

effect of SKI on HG-induced renal tubular cell senescence needs further *in vivo* exploration.

Acknowledgements

This study was supported by the National Natural Science Fundation of China (Nos. 81470962, 81670661, and 81400733); the medical research funding of PLA (No. AWS14C003); and the National Science and Technology Support Plan (No. 2015BAI12B06). We thank Prof. Jianxin Jiang (Key Laboratory of Trauma, Burns and Combined Injury, Institute of Surgery Research, Daping Hospital, Army Medical University, Chongqing, China) for his technical assistance and instructions.

Compliance with ethics guidelines

Biqiong Fu, Jie Yang, Jia Chen, Lirong Lin, Kehong Chen, Weiwei Zhang, Jianguo Zhang, and Yani He declare that they have no conflicts of interest. All experiment were approved by the Army Medical University experiment animal administrative committee. All institutional and national guidelines for the care and use of laboratory animals were followed.

References

1. Muñoz-Espín D, Serrano M. Cellular senescence: from physiology to pathology. Nat Rev Mol Cell Biol 2014; 15(7): 482–496
2. Verzola D, Gandolfo MT, Gaetani G, Ferraris A, Mangerini R, Ferrario F, Villaggio B, Gianiorio F, Tosetti F, Weiss U, Traverso P, Mji M, Deferrari G, Garibotto G. Accelerated senescence in the kidneys of patients with type 2 diabetic nephropathy. Am J Physiol Renal Physiol 2008; 295(5): F1563–F1573
3. Ruggenenti P, Remuzzi G. Nephropathy of type-2 diabetes mellitus. J Am Soc Nephrol 1998; 9(11): 2157–2169
4. Rodier F, Campisi J. Four faces of cellular senescence. J Cell Biol 2011; 192(4): 547–556
5. van Deursen JM. The role of senescent cells in ageing. Nature 2014; 509(7501): 439–446
6. Vallon V. The proximal tubule in the pathophysiology of the diabetic kidney. Am J Physiol Regul Integr Comp Physiol 2011; 300 (5): R1009–R1022
7. Menini S, Amadio L, Oddi G, Ricci C, Pesce C, Pugliese F, Giorgio M, Migliaccio E, Pelicci P, Iacobini C, Pugliese G. Deletion of p66Shc longevity gene protects against experimental diabetic glomerulopathy by preventing diabetes-induced oxidative stress. Diabetes 2006; 55(6): 1642–1650
8. Ning ZQ. Qiao Y, Bai J, Wang JW, Huang XF, Zhao X, Xu HC, Wen AD. Treatment of early diabetic nephropathy with Shenkang injection: a meta-analysis. J Shanxi College Trad Chin Med (Shanxi Zhong Yi Xue Yuan Xue Bao) 2014; 37: 39–43 (in Chinese)
9. Jiang ZW, Lu YY, Xia JL. The phase IV clinical observation study of Shenkang injection on chronic renal failure. J China Med Univ (Zhongguo Yi Ke Da Xue Xue Bao) 2011; 40(10): 941–945 (in Chinese)
10. Yong Z, Yang R, Chen J. Shenkang injection in the treatment of diabetic nephropathy meta-analysis. J Liaoning Univ Trad Chin Med (Liaoning Zhong Yi Yao Da Xue Xue Bao) 2015; 17: 165–167 (in Chinese)
11. Wu X, Guan Y, Yan J, Liu M, Yin Y, Duan J, Wei G, Hu T, Weng Y, Xi M, Wen A. Shenkang injection suppresses kidney fibrosis and oxidative stress via transforming growth factor-β/Smad3 signalling pathway *in vivo* and *in vitro*. J Pharm Pharmacol 2015; 67(8): 1054–1065
12. Du J, Chen H, Wang X. Song L, He YH, Ye CH. Effect of Shengkang injection on hypertrophy and expression of p21 and p27 in glomerular mesangial cells of rats cultured in high glucose. Chin J Integr Trad West Med (Zhongguo Zhong Xi Yi Jie He Za Zhi) 2006; 26: 68–71 (in Chinese)
13. Yao S, Zhang J, Wang D, Hou J, Yang W, Da J, Cai L, Yang M, Jiang B, Liu X, Guo D, Wu W. Discriminatory components retracing strategy for monitoring the preparation procedure of Chinese patent medicines by fingerprint and chemometric analysis. PLoS One 2015; 10(3):e0121366
14. Terryn S, Jouret F, Vandenabeele F, Smolders I, Moreels M, Devuyst O, Steels P, Van Kerkhove E. A primary culture of mouse proximal tubular cells, established on collagen-coated membranes. Am J Physiol Renal Physiol 2007; 293(2): F476–F485
15. Breggia AC, Himmelfarb J. Primary mouse renal tubular epithelial cells have variable injury tolerance to ischemic and chemical mediators of oxidative stress. Oxid Med Cell Longev 2008; 1(1): 33–38
16. Kroening S, Neubauer E, Wullich B, Aten J, Goppelt-Struebe M. Characterization of connective tissue growth factor expression in primary cultures of human tubular epithelial cells: modulation by hypoxia. Am J Physiol Renal Physiol 2010; 298(3): F796–F806
17. Satriano J, Mansoury H, Deng A, Sharma K, Vallon V, Blantz RC, Thomson SC. Transition of kidney tubule cells to a senescent phenotype in early experimental diabetes. Am J Physiol Cell Physiol 2010; 299(2): C374–C380
18. Navarro-González JF, Mora-Fernández C, Muros de Fuentes M, García-Pérez J. Inflammatory molecules and pathways in the pathogenesis of diabetic nephropathy. Nat Rev Nephrol 2011; 7 (6): 327–340
19. Braun H, Schmidt BMW, Raiss M, Baisantry A, Mircea-Constantin D, Wang S, Gross ML, Serrano M, Schmitt R, Melk A. Cellular senescence limits regenerative capacity and allograft survival. J Am Soc Nephrol 2012; 23(9): 1467–1473
20. Vallon V, Thomson SC. Renal function in diabetic disease models: the tubular system in the pathophysiology of the diabetic kidney. Annu Rev Physiol 2012; 74(1): 351–375
21. Stenvinkel P, Larsson TE. Chronic kidney disease: a clinical model of premature aging. Am J Kidney Dis 2013; 62(2): 339–351
22. Tchkonia T, Zhu Y, van Deursen J, Campisi J, Kirkland JL. Cellular senescence and the senescent secretory phenotype: therapeutic opportunities. J Clin Invest 2013; 123(3): 966–972
23. Zhang YU, Zhou N, Wang H, Wang S, He J. Effect of Shenkang granules on the progression of chronic renal failure in 5/6 nephrectomized rats. Exp Ther Med 2015; 9(6): 2034–2042
24. Molgora B, Bateman R, Sweeney G, Finger D, Dimler T, Effros RB, Valenzuela HF. Functional assessment of pharmacological telomerase activators in human T cells. Cells 2013; 2(1): 57–66
25. Hu G, Liu J, Zhen YZ, Xu R, Qiao Y, Wei J, Tu P, Lin YJ. Rhein

lysinate increases the median survival time of SAMP10 mice: protective role in the kidney. Acta Pharmacol Sin 2013; 34(4): 515–521

26. Camici GG, Schiavoni M, Francia P, Bachschmid M, Martin-Padura I, Hersberger M, Tanner FC, Pelicci P, Volpe M, Anversa P, Lüscher TF, Cosentino F. Genetic deletion of p66(Shc) adaptor protein prevents hyperglycemia-induced endothelial dysfunction and oxidative stress. Proc Natl Acad Sci USA 2007; 104(12): 5217–5222
27. Trinei M, Berniakovich I, Beltrami E, Migliaccio E, Fassina A, Pelicci P, Giorgio M. P66Shc signals to age. Aging (Albany NY) 2009; 1(6): 503–510
28. Kitada M, Kume S, Takeda-Watanabe A, Kanasaki K, Koya D. Sirtuins and renal diseases: relationship with aging and diabetic nephropathy. Clin Sci (Lond) 2013; 124(3): 153–164
29. Asai O, Nakatani K, Tanaka T, Sakan H, Imura A, Yoshimoto S, Samejima K, Yamaguchi Y, Matsui M, Akai Y, Konishi N, Iwano M, Nabeshima Y, Saito Y. Decreased renal α-Klotho expression in early diabetic nephropathy in humans and mice and its possible role in urinary calcium excretion. Kidney Int 2012; 81(6): 539–547
30. Yang HC, Deleuze S, Zuo Y, Potthoff SA, Ma LJ, Fogo AB. The PPARγ agonist pioglitazone ameliorates aging-related progressive renal injury. J Am Soc Nephrol 2009; 20(11): 2380–2388
31. Lin Y, Kuro-o M, Sun Z. Genetic deficiency of anti-aging gene klotho exacerbates early nephropathy in STZ-induced diabetes in male mice. Endocrinology 2013; 154(10): 3855–3863
32. Xu S, Cai Y, Wei Y. mTOR signaling from cellular senescence to organismal aging. Aging Dis 2013; 5(4): 263–273
33. Kume S, Kitada M, Kanasaki K, Maegawa H, Koya D. Anti-aging molecule, Sirt1: a novel therapeutic target for diabetic nephropathy. Arch Pharm Res 2013; 36(2): 230–236
34. He W, Wang Y, Zhang MZ, You L, Davis LS, Fan H, Yang HC, Fogo AB, Zent R, Harris RC, Breyer MD, Hao CM. Sirt1 activation protects the mouse renal medulla from oxidative injury. J Clin Invest 2010; 120(4): 1056–1068
35. Kim MK, Chung SW, Kim DH, Kim JM, Lee EK, Kim JY, Ha YM, Kim YH, No JK, Chung HS, Park KY, Rhee SH, Choi JS, Yu BP, Yokozawa T, Kim YJ, Chung HY. Modulation of age-related NF-κB activation by dietary zingerone via MAPK pathway. Exp Gerontol 2010; 45(6): 419–426
36. Yamagishi T, Saito Y, Nakamura T, Takeda S, Kanai H, Sumino H, Kuro-o M, Nabeshima Y, Kurabayashi M, Nagai R. Troglitazone improves endothelial function and augments renal klotho mRNA expression in Otsuka Long-Evans Tokushima Fatty (OLETF) rats with multiple atherogenic risk factors. Hypertens Res 2001; 24(6): 705–709
37. Zhang H, Li Y, Fan Y, Wu J, Zhao B, Guan Y, Chien S, Wang N. Klotho is a target gene of PPAR-γ. Kidney Int 2008; 74(6): 732–739
38. Speeckaert MM, Vanfraechem C, Speeckaert R, Delanghe JR. Peroxisome proliferator-activated receptor agonists in a battle against the aging kidney. Ageing Res Rev 2014; 14: 1–18
39. Blagosklonny MV. TOR-centric view on insulin resistance and diabetic complications: perspective for endocrinologists and gerontologists. Cell Death Dis 2013; 4(12): e964